J Biol Inorg Chem (2010) 15:889–902
DOI 10.1007/s00775-010-0652-z

ORIGINAL PAPER

Role of oxidative stress in the antitumoral action of a new vanadyl(IV) complex with the flavonoid chrysin in two osteoblast cell lines: relationship with the radical scavenger activity

Luciana Naso · Evelina Gloria Ferrer · Luis Lezama · Teófilo Rojo · Susana Beatriz Etcheverry · Patricia Williams

Received: 25 November 2009 / Accepted: 7 March 2010 / Published online: 4 April 2010
© SBIC 2010

Abstract The new complex $[VO(chrysin)_2EtOH]_2$ (VOchrys) has been synthesized and thoroughly characterized. Fourier transform IR, UV–vis, diffuse reflectance, and EPR spectroscopies as well as elemental analysis and thermal measurements were performed. In solution, different species could be detected by EPR spectroscopy as a function of the ligand-to-metal ratio. The stoichiometry of the chelate complex formed at pH 5 was also determined by spectrophotometric titrations. Since flavonoids are natural antioxidant compounds, the antioxidant capacity of chrysin and its vanadyl(IV) complex was investigated using different radicals. Chrysin and its complex were not able to diminish the level of superoxide and 1,1-diphenyl-2-picrylhydrazyl radicals to a great extent. In contrast, they were strong scavengers for 2,2′-azinobis(3-ethylbenzothiazoline-6-sulfonic acid diammonium salt radical cations and OH· radicals with a greater potency for VOchrys. Taking into account their selective antioxidant properties, we investigated the bioactivity of these compounds in two osteoblast-like cells in culture. Chrysin and VOchrys caused an inhibition of cell proliferation in MC3T3E1 normal osteoblasts and UMR106 tumor cells in a dose-response manner, with a greater effect in the latter cell line. The generation of reactive oxygen species (ROS) was evaluated in both cell lines and a correlation could be established between the antiproliferative effects of chrysin and the increase in the ROS levels. The complex did not generate types of ROS that can be detected by the dihydrorhodamine 123 technique so the antiproliferative effect may be attributed to the formation of other radicals such as superoxide, which is not detected by this probe. The morphological alterations were in agreement with these changes.

Keywords Chrysin · Oxidovanadium(IV) · Reactive oxygen species · Scavenger activity · Osteoblasts

Abbreviations

ABTS	2,2′-Azinobis(3-ethylbenzothiazoline-6-sulfonic acid) diammonium salt
DHR123	Dihydrorhodamine 123
DMEM	Dulbecco's modified Eagle's medium
DMSO	Dimethyl sulfoxide
DPPH·	1,1-Diphenyl-2-picrylhydrazyl radical
FBS	Fetal bovine serum
NBT	Nitroblue tetrazolium
PBS	Phosphate-buffered saline
ROS	Reactive oxygen species
SOD	Superoxide dismutase
TEAC	Trolox equivalent antioxidant coefficient
VOchrys	$[VO(chrysin)_2EtOH]_2$

Electronic supplementary material The online version of this article (doi:10.1007/s00775-010-0652-z) contains supplementary material, which is available to authorized users.

L. Naso · E. G. Ferrer · S. B. Etcheverry · P. Williams (✉)
Facultad de Ciencias Exactas,
Centro de Química Inorgánica (CEQUINOR/CONICET, UNLP), Universidad Nacional de La Plata,
C. Correo 962, 1900 La Plata, Argentina
e-mail: williams@quimica.unlp.edu.ar

L. Lezama · T. Rojo
Departamento de Química Inorgánica,
Facultad de Ciencia y Tecnología,
Universidad del País Vasco,
Apdo 644, 48080 Bilbao, Spain

S. B. Etcheverry
Cátedra de Bioquímica Patológica,
Facultad de Ciencias Exactas,
Universidad Nacional de La Plata,
47 y 115, 1900 La Plata, Argentina

Introduction

Polyphenolic flavonoids are substances isolated from a wide range of vascular plants. The family includes monomeric flavanols, flavanones, anthocyanidins and flavones. The biological, pharmacological, and medicinal properties of the flavonoids are well known [1, 2]. They act in plants as antioxidants, antimicrobials, photoreceptors, visual attractors, feeding repellants, and for light screening. Many studies have suggested that flavonoids exhibit biological activities, including antiallergenic, antiviral, antiinflammatory, antitumoral, and vasodilating actions and estrogenic effects, as well as being inhibitors of phospholipase A, cyclooxygenase, and lipoxygenase, glutathione reductase, and xanthine oxidase. So, the dietary intake of these natural products is considered very important for preventing a wide variety of diseases which involve free-radical-mediated damage in disease-generating processes [3–6]. Most of the interest has been devoted to the antioxidant activity of flavonoids, which is due to their ability to reduce free-radical formation and to scavenge free radicals. This activity depends mainly on the flavonoid structure. These substances have the 2-phenylbenzo-γ-pyrone ($C_6O_3C_6$) skeleton. Chrysin, 5,7-dihydroxy-2-phenyl-4*H*-chromen-4-one (Fig. 1), is a naturally occurring flavone extracted from blue passion flower and present in honeycomb [7].

Chrysin is one of the lesser known flavonoids and, like other members of this group, is insoluble in water. It has been found that flavonoids have three structural configurations that facilitate their radical-scavenging capability: (1) the presence of a catechol group in ring B, (2) a 2,3-double bond conjugated with the 4-oxido group, and (3) the presence of a 3-hydroxyl group in the heterocyclic ring, C [8]. In this context, the antioxidant effects of chrysin are of medium intensity owing to the absence of a catechol group in ring B and a 3-hydroxyl group in the heterocyclic ring. These parameters are also consistent with the antioxidant activity of the 5,7-metadihydroxy arrangement of the A ring [1].

A number of flavonoids efficiently chelate trace metals, which play an important role in oxygen metabolism. According to the structure of chrysin, the metal chelation site is unique (5-hydroxy and 4-carbonyl groups in the C ring). The antitumoral effect of chrysin on four different tumor cell lines was reported. Murine cell lines (LM3, mammary adenocarcinoma; B16-F0, melanoma) and human cell lines (HeLa, cervical adenocarcinoma; KB, oropharyngeal carcinoma) treated with 20 μM chrysin undergo the inhibition of more than 50% of cell proliferation [9]. But at the same concentration, there were no cytotoxic effects on epithelial cells derived from normal mammary gland of mice (NMuMG) or fibroblastic cells from mouse embryo (3T3).

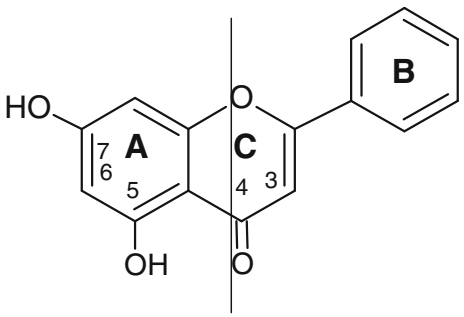

Fig. 1 Chrysin. *Ring B* cynnamoyl system, *ring A* benzoyl system

Coordination complexes of transition metals and chrysin are scarcely reported in the literature. Chrysinate complexes have been synthesized and characterized with lanthanide(III) [10], Al(III), Ga(III), In(III) [11], Co(II), Ni(II), Cu(II) [12], Zn(II), Ti(IV), and Zr(IV) [13] but their biological properties were not examined. It is well known that vanadium compounds show interesting biological effects both in vivo and in vitro. Vanadium promotes glucose transport and metabolism, lipid, DNA, and protein synthesis, and also has mitogenic effects in different cell types. Several vanadium compounds show potential pharmacological activity mainly as insulin mimics and antitumoral and osteogenic agents. As part of our project devoted to the investigation of new vanadium derivatives with potential therapeutic applications, we have selected several flavonoids with different activities, and particularly in the work reported here the behavior of the chrysin–vanadyl(IV) system has been investigated.

The synthesis and characterization of the vanadyl–chrysinate complex and the determination of the possible improvement of the antioxidant and antitumoral properties of the flavonoid are reported.

Materials and methods

Materials

Chrysin (Sigma), vanadyl acetylacetonate (Fluka), vanadyl sulfate pentahydrate (Merck), and sodium methoxide (Fluka) were used as supplied. Corning or Falcon provided tissue culture materials. Dulbecco's modified Eagle's medium (DMEM), and trypsin–EDTA were purchased from Gibco (Gaithersburg, MD, USA) and fetal bovine serum (FBS) was purchased from GibcoBRL (Life Technologies, Germany). All other chemicals used were of analytical grade.

Physicochemical characterization

The electronic UV–vis spectra were recorded with a Hewlett-Packard 8453 diode-array spectrophotometer. The

diffuse reflectance spectrum was recorded with a Shimadzu UV-300 spectrophotometer, using MgO as a standard. Infrared spectra were recorded with a Bruker IFS 66 Fourier transform infrared spectrophotometer from 4,000 to 400 cm^{-1} using the KBr pellet technique. Thermogravimetric analysis and differential thermal analysis were performed with Shimadzu systems (models TG-50 and DTA-50, respectively), working in an oxygen flow of 50 mL/min and at a heating rate of 10 K/min. Sample quantities ranged between 10 and 20 mg. Al_2O_3 was used as a differential thermal analysis standard. A Bruker ESP300 spectrometer operating at X- and Q-bands and equipped with standard Oxford Instruments low-temperature devices (ESR900/ITC4) was used to record the spectra of the compounds at different temperatures. Anisotropic X-band EPR spectra of frozen solutions were recorded at 140 K, after addition of 5% dimethyl sulfoxide (DMSO) to ensure good glass formation. A computer simulation of the EPR spectra was performed using the program WINEPR SimFonia version 1.25 (Bruker Analytische Messtechnik, 1996). Elemental analysis for carbon and hydrogen was performed using a Carlo Erba EA 1108 analyzer. Vanadium content was determined by the tungstophosphovanadic method [14].

Synthesis of $[VO(chrysin)_2EtOH]_2$

Chrysin (0.5 mmol) was mixed with vanadyl acetylacetonate (0.25 mmol) in absolute ethanol and refluxed during 1.30 h. The final pH value was 5. The resulting hot, green suspension was filtered off, and the solid was washed three times with absolute ethanol, and air-dried. Anal. calcd. for $C_{64}H_{48}O_{20}V_2$: C 62.0, H 3.9, V 8.2; found: C 61.9, H 4.0, V 8.3; yield: 71%. UV–vis data for 1:2 VO to chrysin, pH 5, ethanol: 576 nm ($3d_{xy} \rightarrow 3d_{x^2-y^2}$, $\varepsilon = 12.0\,M^{-1}\,cm^{-1}$); 794 nm ($3d_{xy} \rightarrow 3d_{xz}, 3d_{yz}$, $\varepsilon = 27.7\ M^{-1}\ cm^{-1}$). The ethanol content was additionally confirmed by the thermogravimetric measurements. Thermogravimetric analysis (oxygen atmosphere, flux velocity, 50 mL/min): in a first step (293–466 K) one ethanol molecule was lost ($\Delta w_{calcd.}$ 7.43%, Δw_{found} 7.54%). The final residue up to 1,273 K was characterized by infrared spectroscopy as V_2O_5. The weight of the final residue was 14.70%, in agreement with the theoretical value. Reflectance spectrum: 580 nm (sh), 650 nm.

Spectrophotometric titrations

The stoichiometry of the complex was determined by the molar ratio method. An ethanolic solution of chrysin (4×10^{-5} M) was prepared and its electronic spectrum recorded. The absorption spectra of different ethanolic solutions of 4×10^{-5} M chrysin and $VOSO_4 \cdot 5H_2O$ in ligand-to-metal molar ratios from 10 to 0.5 (pH 5) were measured.

Antioxidant properties

1,1-Diphenyl-2-picrylhydrazyl assays

The antiradical activity of chrysin and $[VO(chrysin)_2EtOH]_2$ (VOchrys) was measured in triplicate using a modified Yamaguchi et al. [15] method. A methanolic solution of 1,1-diphenyl-2-picrylhydrazyl radical (DPPH·) (4 mL, 40 ppm) was added to 1 mL of the antioxidant solutions in 0.1 M tris(hydroxymethyl)aminomethane–HCl buffer (pH 7.1) at 298 K, giving final concentrations of 10, 25, 50, and 100 μM. From the UV–vis spectra, the absorbance at 517 nm was measured after 60 min of the reaction in the dark and compared with the absorbance of control prepared in a similar way without the addition of the antioxidants (this value was assigned arbitrarily as 100).

2,2′-Azinobis(3-ethylbenzothiazoline-6-sulfonic acid) diammonium salt decoloration assay

The total antioxidant activity was measured using the Trolox (6-hydroxy-2,5,7,8-tetramethylchroman-2-carboxylic acid) equivalent antioxidant coefficient (TEAC). The radical cation of 2,2′-azinobis(3-ethylbenzothiazoline-6-sulfonic acid) diammonium salt (ABTS) was generated by incubating ABTS with potassium persulfate. Chemical compounds that inhibit the potassium persulfate activity may reduce the production of $ABTS^{\cdot+}$. This reduction results in a decrease of the total $ABTS^{\cdot+}$ concentration in the system and contributes to the total $ABTS^{\cdot+}$ scavenging capacity. Briefly, an aqueous solution of ABTS (0.25 mM) and potassium persulfate (0.04 mM) was incubated in the dark for 24 h. The solution was then diluted five times in 0.1 M KH_2PO_4–NaOH buffer (pH 7.4). To 990 μL of this mixture, 10 μL of chrysin, the complex, or the Trolox standard in phosphate buffer was added (final concentrations 0–100 μM). The reduction of $ABTS^{\cdot+}$ was monitored spectrophotometrically 6 min after the initial mixing at 298 K. The percentage decrease of the absorbance of the band at 734 nm was calculated considering that the basal condition (without antioxidant additions) had been assigned as 100% and was plotted as a function of the concentration of the samples giving the total antioxidant activity. The TEAC was calculated from the slope of the plot of the percentage inhibition of absorbance versus the concentration of the antioxidant divided by the slope of the plot for Trolox [16, 17].

Superoxide dismutase assays

The superoxide dismutase (SOD) activity was examined indirectly using the nitroblue tetrazolium (NBT) assay. The indirect determination of the activity of chrysin and the

vanadium complex was assayed by their ability to inhibit the reduction of NBT by the superoxide anion generated by the phenazine methosulfate and reduced nicotinamide adenine dinucleotide system. As the reaction proceeded, the formazan color developed and a change from yellow to blue was observed which was associated with an increase of the intensity of the band at 560 nm in the absorption spectrum. The system contained 0.5 mL of sample, 0.5 mL of 1.40 mM reduced nicotinamide adenine dinucleotide, and 0.5 mL of 300 μM NBT, in 0.1 M KH_2PO_4–NaOH buffer (pH 7.5). After incubation at 298 K for 15 min, the reaction was started by adding 0.5 mL of 120 μM phenazine methosulfate [18]. Then, the reaction mixture was incubated for 5 min. Each experiment was performed in triplicate and at least three independent experiments were performed in each case. The amount of complex (or chrysin) that gave a 50% inhibition (IC_{50}) was obtained by plotting the percentage of inhibition versus the log of the concentration of the solution tested.

Scavenging of the hydroxyl radical

Hydroxyl radicals were generated by the ascorbate–iron–H_2O_2 system. Briefly, the reaction mixture contained 3.75 mM 2-deoxyribose, 2.0 mM H_2O_2, 100 μM $FeCl_3$, and 100 μM EDTA without or with test compound in 20 mM KH_2PO_4–KOH buffer, pH 7.4. The reaction was triggered by the addition of 100 μM ascorbate and the mixture was incubated at 310 K for 30 min. Solutions of $FeCl_3$, ascorbate, and H_2O_2 were made up in deaerated water immediately before use. The extent of deoxyribose degradation by hydroxyl radical was measured with the thiobarbituric acid method [19, 20].

Cell culture

MC3T3E1 osteoblastic mouse calvarium-derived cells and UMR106 rat osteosarcoma-derived cells were grown in DMEM supplemented with 100 U/mL penicillin, 100 μg/mL streptomycin, and 10% (v/v) FBS at 310 K, 5% CO_2. When 70–80% confluence was reached, cells were subcultured using 0.1% trypsin 1 mM EDTA in Ca(II)–Mg(II)-free phosphate-buffered saline (PBS) (11 mM KH_2PO_4, 26 mM Na_2HPO_4, 115 mM NaCl, pH 7.4). For experiments, cells were grown in multiwell plates. When cells reached 70% confluence, the monolayers were washed twice with DMEM and were incubated in different conditions depending on the experiments.

Biological assays

Cell proliferation, reversibility assay, and cell morphology experiments were performed with VO(IV), the complex, and the free ligand. Intracellular formation of reactive oxygen species (ROS) was also determined. Briefly, the cell proliferation was assessed by the crystal violet bioassay. Stock complex solutions were prepared by dissolving VOchrys in DMSO with a manipulation time of 5 min. Then, the solution of the complex was immediately diluted with DMEM. The maximum concentration of DMSO in DMEM was always lower than 0.5%, being innocuous for the cultures. Then, the complex solution was added to the cells in different concentrations and the cells were incubated for 24 h. It is important to note that the dissolution in DMSO leads to the monomeric complex (the same EPR parameters as those for methanol solution were obtained), without oxidation or reduction of the metal cation. The complex remains stable in a DMSO solution (no changes were observed in the UV–vis spectra) during its manipulation for biological studies. The cells in culture were stained with crystal violet after the incubation period. Next, they were washed to remove the excess of dye. The crystal violet taken up by the osteoblasts was extracted with the appropriate buffer and the absorbance was measured at 540 nm. Previously, a linear correlation was established for the number of cells and the absorbance [21].

The reversibility assay was used to determine the toxicity of an exogenous agent by measuring the viability of the cells after stress incubation. Cells were cultured in 48-well dishes to 70% confluence. Then, they were incubated with different concentrations of VOchrys at 310 K for 24 h. Half of the wells were then used to evaluate cell proliferation by the crystal violet assay. The other 24 wells were washed to eliminate the conditioned medium with the complex and then were incubated with DMEM supplemented with FBS. After that, these cells were incubated for another 24 h at 310 K. Finally, cell proliferation was determined by the crystal violet assay.

Intracellular ROS generation in osteoblast-like cells was measured by oxidation of dihydrorhodamine 123 (DHR123) to rhodamine. Osteoblast-like cells were incubated for 30 min at 310 K in 1.5 mL of Hank's buffered salt solution alone (basal condition) or with chrysin, VOchrys, and VO(IV), in the presence of 10 mM DHR123 [22]. Media were separated and the cell monolayers rinsed with PBS and lysated into 1 mL of 0.1% Triton X-100. The cell extracts were then analyzed for the oxidized product rhodamine by measuring fluorescence (excitation wavelength 500 nm, emission wavelength 536 nm), using a Perkin-Elmer LS 50B spectrofluorometer. The results were corrected for protein content, which was assessed by the method of Bradford [23].

To evaluate the morphology of the cells, they were grown in six-well plates and incubated overnight with fresh serum-free DMEM plus 0 (basal), 50, and 100 μM solutions of the complex. The monolayers were subsequently

washed twice with PBS, fixed with methanol, and stained with 1:10 dilution of Giemsa stain for 10 min [24]. Next, they were washed with water and the morphological changes were examined by light microscopy.

At least three independent experiments were performed for each experimental condition in all the biological assays. The results are expressed as the mean ± the standard error of the mean. Statistical differences were analyzed using the analysis of variance method followed by the test of least significant difference (Fisher).

Solution studies

Electronic spectra

Most flavones and flavonols exhibited two major absorption bands in the UV–vis region [1], band I in the 320–385-nm range representing the B ring (cynnamoyl system) absorption, and band II in the 250–285-nm range representing A ring (benzoyl system, $\pi \rightarrow \pi^*$) absorption. The data were consistent with the recorded observations that an increase in the numbers of hydroxyl groups induced a redshift. The absence of a 3-hydroxyl group in flavones means that band I was always at a wavelength by shorter 20–30 nm than band I in the equivalent flavonols. In the plot shown in Fig. 2 this band is at 314 nm.

Two successive overlapping equilibria could be seen when the pH values were raised. Experimental acid dissociation constants of chrysin have previously been determined using an ethanol–water 50% (w/w) mixture. The values for pK_1 and pK_2 were reported as 7.90 and 11.40, respectively [25]. The pK values in water could not be determined owing to the low solubility of chrysin. However, these values were calculated as 7.1 and 8.4, respectively [26]. The plots in Fig. 2 were obtained for ethanolic solutions.

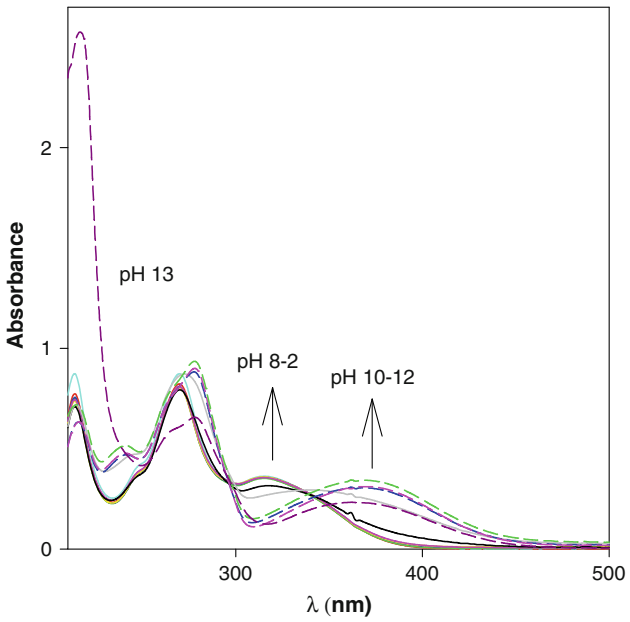

Fig. 2 Spectra of chrysin (4×10^{-5} M), ethanolic solutions, for different pH values: — 2, — 3, — 4, — 5, — 6, — 7, — 8, — 9, --- 10, — 11, --- 12, --- 13

The protonated form gives a maximum at 314 nm that shifted to the red upon addition of the sodium methoxide titrant, giving rise to the monodeprotonated form with a maximum at 365 nm at pH values higher than 8. At pH 13 (adjusted using aqueous 1 M NaOH solution), even though the measurement of these values was not very accurate, the band at 235 nm assigned to the chrysin$^-$ anion vanished, suggesting the formation of the new species chrysin^{2-}.

It is well known that when ligands interact with Lewis acids (such as transition metal cations) their pK_a values are reduced. The interaction of monodeprotonated chrysin with vanadyl(IV) cation could be observed at pH 5 (pH selected for the preparation of the solid). The positions of the spectral bands compared with the positions for the chrys$^-$ species were slightly shifted to the red (242, 280, and 370 nm). The band at 370 nm was assigned to a four C=O and five C–O$^-$ chelation of the ligand [11].

The stoichiometry of the VOchrys system was determined by spectrophotometric titration. Figure 3 showed the spectral patterns of different ligand-to-metal ethanolic chrysin (4×10^{-5} M) solutions, pH 5 (sodium methoxide), under a nitrogen atmosphere.

Starting at a ligand-to-metal ratio od 10:1, the band at 242 nm increased upon addition of different quantities of VO(IV). The molar ratio plot indicated the formation of a 2:1 chrysin–VO complex (Fig. 3, inset). Besides, *d–d* transitions at 576 and 794 nm are observed at a 100-fold concentration, owing to the lower intensity of these absorption bands.

EPR spectra

The spectrophotometric titrations could be followed by EPR spectroscopy to assist in the identification of different vanadium species. EPR spectra illustrating the species formed at various ligand-to-metal ratios, at pH 5, an in ethanol are shown in Fig. 4. For these studies $VOSO_4 \cdot 5H_2O$ was used to obtain free VO(IV) cation able to interact with chrysin.

For ligand-to-metal ratios of 8:1–1:1 only one EPR signal can be observed with the typical eight-line-pattern spectrum for V(IV) systems. These signals indicated the formation of single species (I) in this range. The spectral simulation predicted the formation of a V chromophore with spin Hamiltonian parameters $g_z = 1.949$, $g_x = 1.975$, and $g_y = 1.981$ and hyperfine coupling constants of $A_z = 165.5 \times 10^{-4}$ cm^{-1}, $A_x = 53 \times 10^{-4}$ cm^{-1}, and

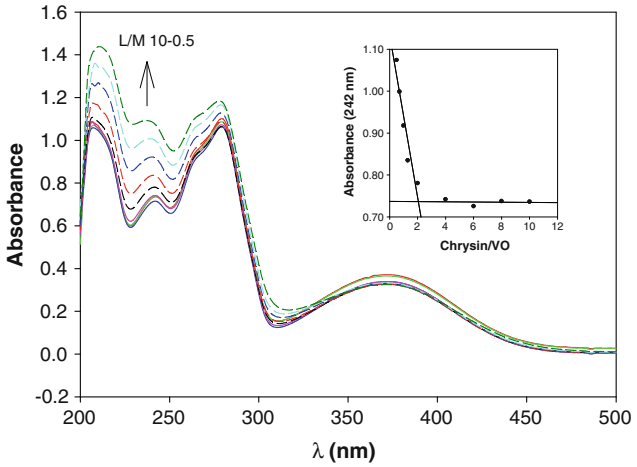

Fig. 3 UV–vis spectra of chrysin (4×10^{-5} M) with the addition of $VOSO_4 \cdot 5H_2O$ in ligand-to-metal ratios (*L/M*) from 10.0 to 0.7 (pH 5); nitrogen atmosphere. The *arrow* indicates increasing metal additions. *Inset*: Spectrophotometric determination of VOchrys complex stoichiometry at 242 nm by the molar ratio method

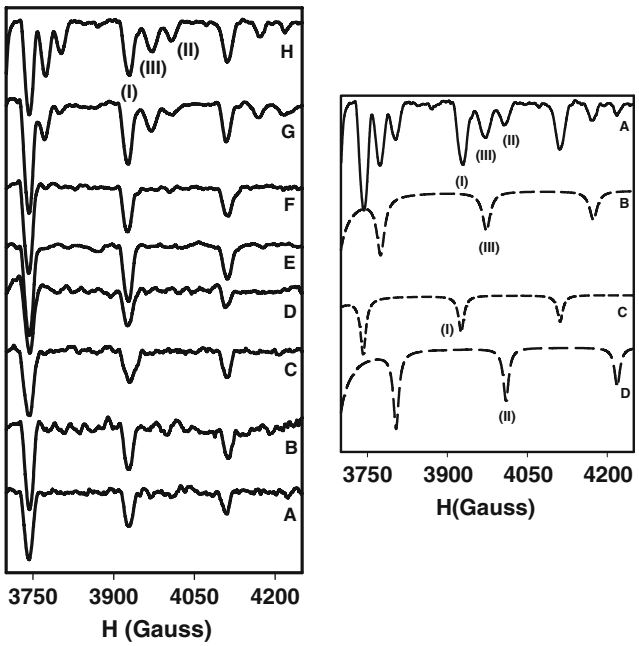

Fig. 4 High-field parallel region of the EPR spectra recorded at 140 K in ethanolic solutions of the $V^{IV}O$ and chrysin system. *Left*: *A* L/M = 8, *B* L/M = 6, *C* L/M = 4, *D* L/M = 2, *E* L/M = 1.3, *F* L/M = 1, *G* L/M = 0.7, *H* L/M = 0.5. *Right*: *A* L/M = 0.5, *B* calculated for species III, *C* calculated for species I, *D* calculated for species II. Total chrysin concentration 1×10^{-3} M

$A_y = 62 \times 10^{-4}$ cm^{-1} ($g_{iso} = 1.968$, $A_{iso} = 93.50 \times 10^{-4}$ cm^{-1}). For ligand-to-metal ratios lower than 1, important variations in the EPR spectra were induced and three signals were observed: the species detected at higher ligand-to-metal ratio were identified as species I and two new species indicated as species II and III, respectively. The signal assigned as II is related to the presence of a species of VO(IV) in ethanol ($g_z = 1.930$, $g_x = 1.980$, $g_y = 1.980$, $A_z = 183 \times 10^{-4}$ cm^{-1}, $A_x = 70 \times 10^{-4}$ cm^{-1}, and $A_y = 70 \times 10^{-4}$ cm^{-1}) ($g_{iso} = 1.963, A_{iso} = 107.7 \times 10^{-4}$ cm^{-1}, own data) and the other one (III) showed that a new paramagnetic species was formed. For the new signal (III), the calculated EPR parameters are $g_z = 1.940$, $g_x = 1.9805$, and $g_y = 1.979$ and the hyperfine coupling constants are $A_z = 177 \times 10^{-4}$ cm^{-1}, $A_x = 65 \times 10^{-4}$ cm^{-1}, and $A_y = 71.5 \times 10^{-4}$ cm^{-1} ($g_{iso} = 1.966, A_{iso} = 104.5 \times 10^{-4}$ cm^{-1}), suggesting the formation of a new complex with modification of the equatorial coordination sphere.

The additivity relationship for VO systems, regarding the magnitude of $A_{\|}$ described by Chasteen [27], can provide some indication of the nature of the equatorial ligands. Using the sum formula, we can calculate the hyperfine component $A_{\|}$ for different ligand compositions:

$$A_z = \sum n_i A_{z,i}$$

n_i being the number of equatorial ligands of type i and $A_{z,i}$ being the contribution to the parallel hyperfine coupling from each of them. The calculated value for different donor group composition can then be compared with the measured hyperfine components. The spin Hamiltonian parameters obtained were in the range usually found for O_4 coordination complexes of the vanadyl ion. Moreover, comparable values were predicted by the above equation considering other complexes with similar donor sets [28–35], and the calculated parameter fitted well in the corresponding $g_{\|}$ versus $A_{\|}$ diagram [36]. Considering the contributions to the parallel hyperfine coupling constant due to the different coordination modes (CO 44.7×10^{-4} cm^{-1} [9]; EtOH 45.7×10^{-4} cm^{-1}, and ArO^- 38.6×10^{-4} cm^{-1} [37, 38], respectively). From the EPR parameters we conclude that the conformation of species I would correspond to a binding mode of 2(CO, O^-) probably including a solvent molecule (ethanol) in the sixth position of the coordination sphere. Using the additivity rule, this assumption gives a calculated value of $A_z = 166.6 \times 10^{-4}$ cm^{-1} (C=O 44.7×10^{-4} cm^{-1}, ArO^- 38.6×10^{-4} cm^{-1}) in good agreement with the values reported for maltol-type ligands assuming *trans* configuration (V=O/solvent) in solution [28, 29, 39]. For species III, we presume one equatorial (C=O, O^-) ligand set, which is in accordance with the reported experimental data for metal complexes coordinated to only one ligand, VOL [30, 39]. These assignments could also been confirmed by the disappearance of species II and III in excess of ligand [30]. These results are in accordance with the spectrophotometric titrations suggesting the formation of VOL_2 as the main species in solution. It is worth pointing out that these results cannot unambiguously be transcribed to the vanadium speciation

in the bioassays because in these studies solutions prepared by dissolving the solid complex in DMSO were used (see later).

Solid characterization of the complex

Infrared spectra

The infrared spectra data for chrysin and the oxidovanadium(IV) complex, in the most interesting spectral range, between 1,700 and 900 cm^{-1}, are presented in Table 1.

The assignments were performed according to general [40, 41] and particular [42] references, and by comparison with the previously investigated VO^{2+}–flavonoid complexes [43, 44].

The major changes in the infrared spectrum upon coordination are:

- The C=O stretching band is shifted to lower energies owing to the increase in length of the C=O bond coordinated to vanadyl(IV).
- The deprotonation and coordination to O(5) is indicated by the presence of the bands at 1,596, 1,351, and 1,247 cm^{-1}.
- The modifications of rings A and C were detected by the displacements of the bands at 1,616, 1,580, and 1,360 cm^{-1}, indicating an alteration of the ring structure [45].
- The band corresponding to the vibrations of ring B at 1,097 cm^{-1} was not affected by the interaction of chrysin with the metal center.
- The position of the V=O stretching band is distinctive for an oxygenated coordination sphere.

Table 1 Assignment of the main bands of the infrared spectra of chrysin and the vanadyl(IV) complex, VOchrys (band positions in reciprocal centimeters)

Chrysin	VOchrys	Assignments
1,665 vs	1,629 s	ν(C=O)
1,616 s	1,596 s	ν(C=O), $\nu(C_2{=}C_3)$, ring A quinoid str
1,580 m		δ(5OH), δ(7OH), ring A quinoid str
1,490 m	1,520 vs	Ring B, δ_{ip}(CH)
1,450 m	1,426 s	δ(7OH), δ_{ip}(C8H)
1,362 vs	1,351 s	Ring A, C trigonal str, δ(5OH), δ(7OH)
1,239 m	1,247 m	δ_{ip}(C3H), δ(5OH), δ(7OH)
1,167 vs	1,162 vs	Ring B, δ_{ip}(CH)
1,097 m	1,097 m	δ_{ip}(COC), δ_{ip}(CH)
1,034 m	1,034 m	δ_{ip}(CH)
	968 m	ν(V=O)

vs very strong, *s* strong, *m* medium

EPR spectrum

With the aim to obtain deeper insight into the environment around vanadium(IV) ion in the complex, EPR spectroscopy measurements were obtained. The spectrum was obtained working with the microcrystalline powder at room temperature, X-band (Fig. 5, spectrum A).

The multiline features of the spectrum with a broad underlying envelope around 3,500 G were due to $\Delta M_s = \pm 1$ transitions of the dimeric species. This spectrum was typical of a triplet state, indicating the presence of two interacting VO^{2+} nuclei with spin ½ giving a singlet $S = 0$ and a triplet $S = 1$ state. Some other signals were also observed, corresponding to the hyperfine structure of V(IV) isolated species (100% abundant ^{51}V nucleus with $I = 7/2$) and might have originated from the presence of monomeric impurities. The parallel and perpendicular parts overlapped extensively because of the similarity of $g_{\|}$ and $g_{\perp}$. The sets of lines in the perpendicular region were separated by the zero-field splitting parameter D, whereas the parallel sets were separated by $2D$. Unfortunately the $\Delta M_s = \pm 2$ transition was not observed. In spite of the superimposition of the different components and from the spectral analysis of the resonances of the dimer, the spin Hamiltonian parameters of the main contribution could be estimated by comparing the room-temperature spectrum with spectra generated by a computer simulation program working at the second order of perturbation theory.

The calculated parameters for the dimer were $g_{\|} = 1.943$, $g_{\perp} = 1.983$, $A_{\|} = 86 \times 10^{-4}$ cm^{-1}, $A_{\perp} = 32 \times 10^{-4}$ cm^{-1}, and $D = 80 \times 10^{-4}$ cm^{-1} (Fig. 5, spectrum B) and for the monomeric impurity were $g_{\|} = 1.943$, $A_{\|} = 173 \times 10^{-4}$ cm^{-1}, $g_{\perp} = 1.983$, and

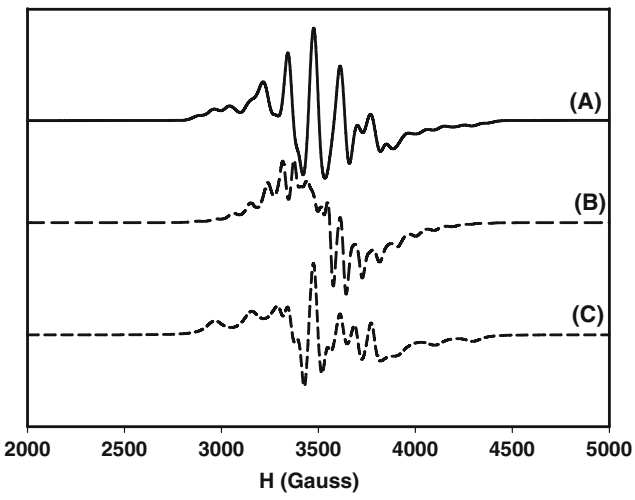

Fig. 5 *A* experimental room-temperature powder EPR spectrum of the $[VO(chrysin)_2EtOH]_2$ (VOchrys) complex measured at X-band (9.87 GHz), *B* spectrum calculated for the dimeric component, and *C* spectrum calculated for the monomeric component

$A_{\perp} = 62 \times 10^{-4}$ cm^{-1} (Fig. 5, spectrum C. In the case of the dimer, the hyperfine splitting value was about half of the estimated value for the vanadyl monomer, as expected.

Considering the additivity relationship, the value of $A_{\parallel}$ obtained is in good agreement with the presence of *cis*-VOL_2(EtOH) and it was comparable with the values reported for VO(IV)–maltol and related systems. That is to say, the equatorial plane is formed by two C=O groups, one ArO^-, and one solvent (ethanol) molecule.

Unfortunately, no structural information from X-ray diffraction analysis on a single crystal is available to determine the binding mode between vanadyl ions for the dimeric species. The formulation of VOchrys as a dimer is based on the observation of a typical EPR spectrum from a triplet state $S = 1$. The following factors support the proposed structure. The agreement between the experimental spectrum (Fig. 5, spectrum A) and the spectrum calculated for the monomeric species (Fig. 5, spectrum C) seems to be better than that between spectra A and B (dimeric signal) in the central part of the spectrum but not in the parallel region (high field), where the overlap is minimized. The hypothesis of an $S = 1$ triplet state with significant zero-field splitting is the only possibility that allows a simultaneous interpretation of the splitting observed in both the X-band and the Q-band with the same set of parameters (see Figs. S1, S2). That the hyperfine constant was about half the estimated value for the vanadyl monomer supports the presence of the dimer. Moreover, the calculation of similar g values for the dimeric and monomeric species implies that both compounds are closely related. Magnetic susceptibility measurements (data not shown) did not reveal appreciable interactions down to 5 K. But, as it is known, the EPR technique is very sensitive for detection of weak magnetic interactions [46, 47] and the observation of a triplet spectrum clearly confirms the presence of an $S = 1$ state. Obviously, the energy gap between the $S = 0$ and $S = 1$ states is probably lower than 1 K. So, considering the extremely weak magnetic coupling detected, an exchange pathway through covalent bonds must be disregarded. The dimerization is probably based on hydrogen bonding, π–π stacking between adjacent units, and/or O=V–O=V interactions, owing to these types of interactions being able to mediate in weak exchange couplings. Furthermore, the detection of an isolated triplet state in the EPR spectra implies the absence of long-range magnetic ordering (chains, planes, or 3D arrangements) in the solid.

Antioxidant properties

From oxidative stability index value measurements it has been found that chrysin displays lower antioxidant activity than other flavonoids [48].

The antiradical activities of flavones, flavanones, and biflavanones in methanolic solution of DPPH· were previously demonstrated by the decoloration test. When antioxidants interact with DPPH·, they transfer one electron or hydrogen atom and thus neutralize its free-radical character. The flavonoids with free hydroxyls only at C-5 and/or at C-7 (5-hydroxyflavone, 7-hydroxyflavone, and 5,7-dihydroxyflavone) had no effect on scavenging these free radicals (1.1%, 33 μM chrysin, methanol). Those with a free hydroxyl at the C-3 position, which were very effective antioxidants, had high ability to scavenge DPPH· (96.5%, morin) [49]. Our experimental results of the scavenging effect with chrysin agreed with the reported values (4%, 25 μM chrysin). Figure 6 shows the results obtained by the DPPH· decoloration test for chrysin and VOchrys. Besides, a 100 μM solution of ascorbic acid (a strong antioxidant agent) was tested as a control of the reaction. In this case, the violet color of DPPH· disappeared immediately, the antiradical activity being 98% (data not shown). The interaction of the flavonoid with the metal produced a high ability to scavenge DPPH· (approximately 45% for 100 μM VOchrys compared with18% for 100 μM chrysin).

As already stated, the catechol structure in the B ring is the major determinant for radical-scavenging capacity of the flavonoids and the removal of the 3-hydroxyl group from ring B reduces the antioxidant capacity. These data were confirmed by the previous measurement of the TEAC. This method assesses the hydrogen-donating ability of

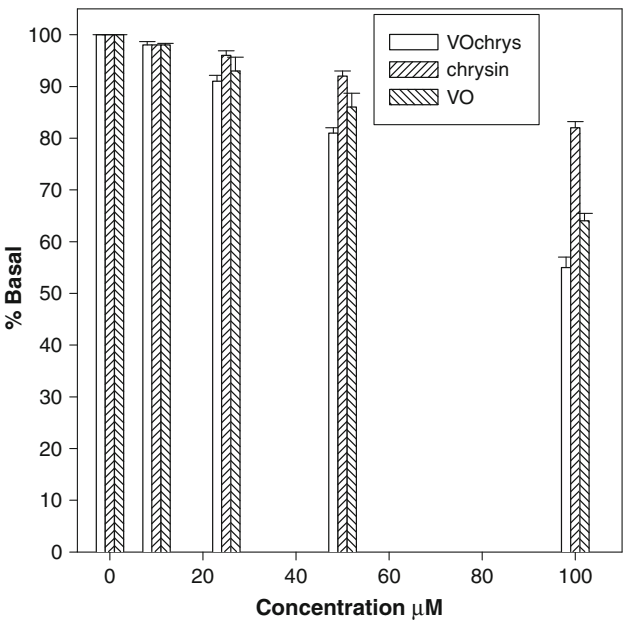

Fig. 6 Effect of chrysin and VOchrys on the reduction of the concentration of 1,1-diphenyl-2-picrylhydrazyl radical. The values are expressed as the mean ± the standard error of at least three independent experiments

flavonoids by evaluating $ABTS^{\cdot+}$ scavenging, and the activity is expressed as the millimolar concentration of Trolox (TEAC) equivalent to the activity of a 1 mM solution of the experimental compound. For chrysin the reported value was 1.4 mM (contribution from the A ring), whereas the activity of the flavonoid quercetin (with an additional hydroxyl group in ring B) was higher, 4.7 mM [2, 50–52]. Our experimental results indicated a value of 0.9 mM for chrysin, being improved by complexation (3.96 mM). It is thus demonstrated that the scavenging power of the ligand was improved by the interaction with the metal center. The result of complexation with oxidovanadium(IV) generated a better scavenging capacity of the complex compared with the free ligand. VOchrys displayed a scavenging power similar to that of quercetin, a flavonoid that has a hydroxyl group in the B ring and whose structure related to the scavenging potential is one of the best among the group of flavonoids as explained already. So, the improvement generated by complexation is similar to the scavenging effect of quercetin. VOchrys behaved as a potent antioxidant like Trolox for $ABTS^{\cdot+}$. To confirm the strong effect of the complexed ligand, measurements at lower concentrations were performed (see Fig. 7). It can be seen that for complex concentrations as low as 1 μM the radical-scavenging capacity is retained (approximately 20% of basal).

Biological free radical reactions generally involve molecular oxygen reduction ultimately yielding ROS, including superoxide anion and hydroxyl radical. ROS are recognized as harmful agents causing strong injuries to several cell components such as lipids, proteins, and DNA, which are gradually damaged [53]. The oxidative injuries caused by ROS are actually acknowledged as active contributors to aging and degenerative diseases, such as brain dysfunction, i.e., Parkinson's and Alzheimer's syndromes [54–56], cardiovascular disorders, and cancer [57, 58].

NBT acts as a superoxide-detection agent through its reduction to formazan. To better emphasize the results, it was convenient to express the SOD activity of the ligand and the complex as IC_{50} values (the concentration of the complex required to attain 50% inhibition of the reduction). The IC_{50} values were obtained by fitting the experimental curves. For VOchrys this value is 157 μM, whereas chrysin practically has no SOD-like activity (Fig. 8) (note that the smaller the IC_{50} value, the higher the SOD activity). Owing to the low solubility of chrysin, data could not be obtained below 1×10^{-4} M. In addition, previously reported IC_{50} values for native enzyme and vanadyl(IV) cation were 0.21 and 15 μM, respectively [44].

It has been demonstrated that for a high superoxide-scavenging activity of flavonoids a hydroxyl group at C-3′ in ring B and at C-3 was essential [52]. In general, an IC_{50} value up to 20 μM is required for a good SOD mimic activity of a compound. It can be seen that the interaction with vanadyl cation improved the scavenging capacity of the ligand for superoxide radicals, but not to an appreciable extent.

Hydroxyl radicals, generated from the ascorbate–iron ion–H_2O_2 system in the presence of ascorbic acid attack deoxyribose to form products that, upon heating with

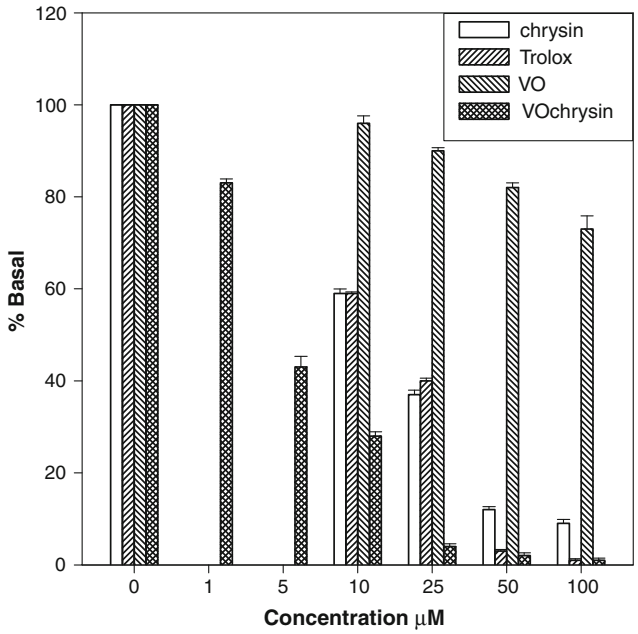

Fig. 7 Total antioxidant activity measured as the reduction of the concentration of $ABTS^{\cdot+}$ by the addition of chrysin, VOchrys, and Trolox. Values are expressed as the mean ± standard error of at least three independent experiments

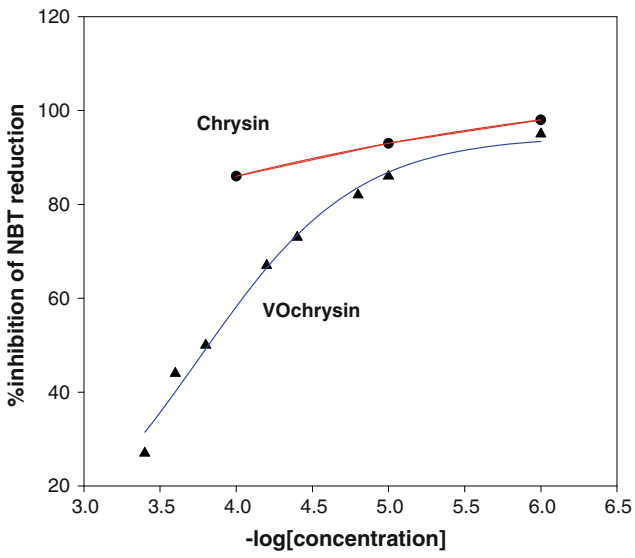

Fig. 8 Effect of chyrsin and VOchrys on reduction of nitroblue tetrazolium by nonenzymatically generated superoxide (phenazine methosulfate and reduced nicotinamide adenine dinucleotide system)

2-thiobarbituric acid under acid conditions, yield a pink chromogen [59]. The ability of VOchrys, chrysin, and VO(IV) to scavenge hydroxyl radicals was measured by the reduction of chromogen formation. The inhibition of color formation was followed by the decrease of the absorption of the UV–vis band at 532 nm [60]. The data for the hydroxyl radical-scavenging activity are shown in Fig. 9.

The inhibitory effect of the complex and its constituents is marked and the average suppression ratio for HO· increases with increasing concentration. The average suppression ratio of VO(IV) is the poorest in all the compounds, and VOchrys is the most effective inhibitor (approximately 75%, 100 μM). For all the radicals tested, the scavenger effect of chrysin was enhanced by coordination to the vanayl(IV) cation. Only for DPPH· were the effects of the ligand and its vanadyl complex comparable.

Proliferation assays

The effects of the complex, the free ligand, and the inorganic vanadyl(IV) cation on osteoblast proliferation can be observed in Fig. 10.

Chrysin and VO(IV) exert the same inhibitory effect in tnormal cells, but the effect of the complex is rather more deleterious at higher concentrations (75 and 100 μM). In tumor cells, VO(IV) does not have any cytotoxic effect on the proliferation [21]. However, chrysin and its vanadyl complex behave as antiproliferative agents (60% inhibition, 100 μM). At approximately 25 μM the antiproliferative

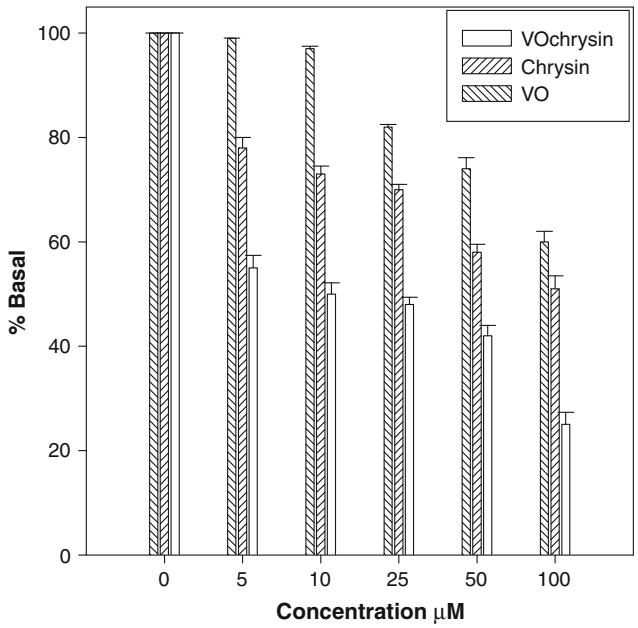

Fig. 9 Effect of VO(IV), chrysin, and VOchrys on the extent of deoxyribose degradation by hydroxyl radical, measured with the thiobarbituric acid method. The values are expressed as the mean ± the standard error of at least three independent experiments

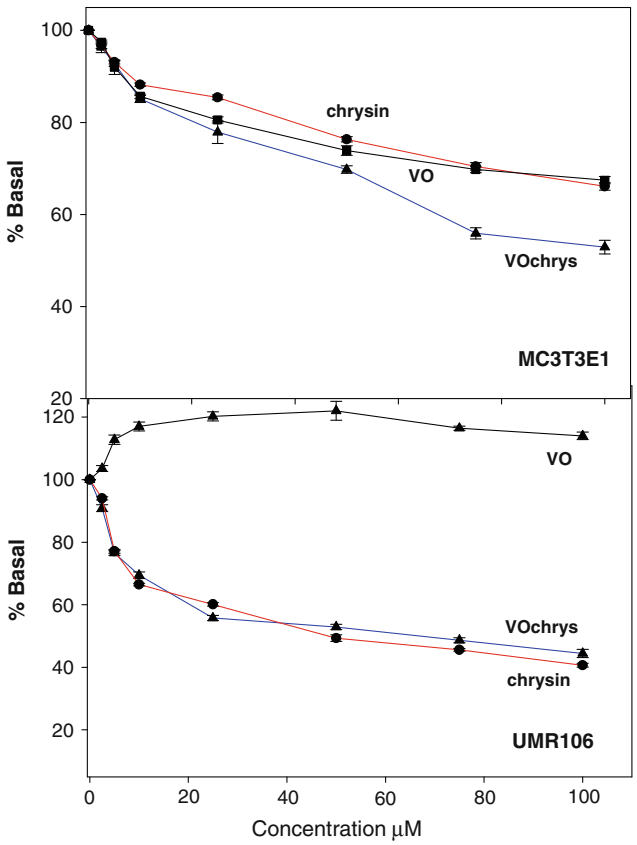

Fig. 10 Effect of chrysin, vanadyl(IV) cation, and VOchrys compounds on UMR106 and MC3T3E1 cell proliferation. Cells were incubated in serum-free Dulbecco's modified Eagle's medium (DMEM) alone (basal) or with different concentrations of the compounds at 310 K for 24 h. The basal values are 8.0×10^4 and 3.8×10^4 cells per well, respectively. The results are expressed as a percentage of the basal level and represent the mean ± the standard error of the mean (SEM; $n = 12$). All results were significant in comparison with the basal level, $P < 0.01$ (except for 2.5 μM in both cell lines)

effect of chrysin in MC3T3E1 is small (approximately 20%) but in the UMR106 tumor cell line it produces about 50% inhibition of proliferation, indicating a behavior comparable with the behavior in other previously tested cell lines [9]. The complexation of the flavonoid practically does not improve its potential pharmacological properties and, on the contrary, it exhibits a higher cytotoxicity in the tumoral osteoblasts.

Reversibility assays

To assess the recovery power of osteoblasts versus the complex-induced shocks, cell viability was determined in the presence of DMEM supplemented with 10% FBS after incubation with increasing concentrations of VOchrys. Figure 11 shows that for UMR106 cells the inhibitory effect of VOchrys was not reversed in any of its cytotoxic concentrations.

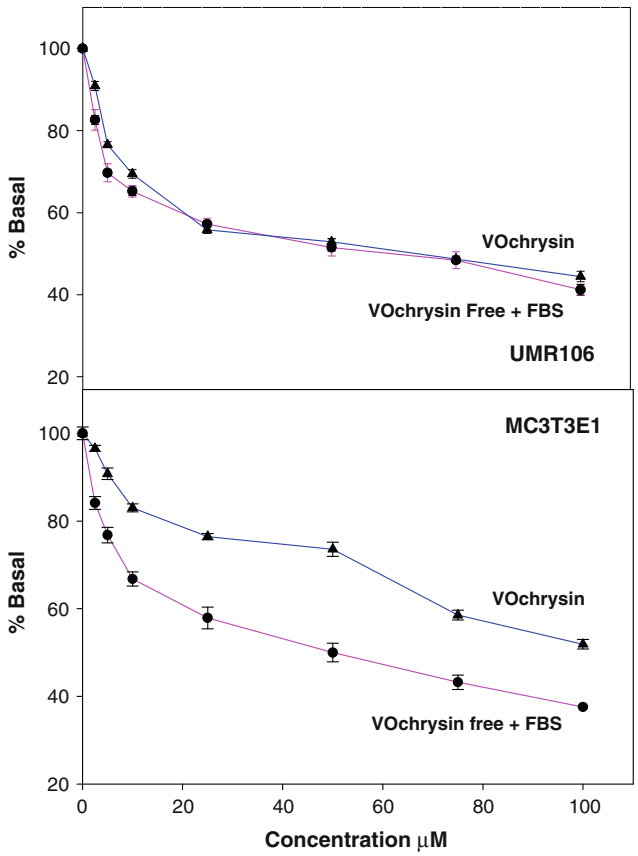

Fig. 11 Cellular proliferation assays and reversibility measurements. Cells incubated with the VOchrys complex for 24 h, under the same conditions as for Fig. 10 (VOchrys). The same cells with removal of the vanadyl compound, treated with DMEM supplemented with fetal bovine serum and incubated for an additional 24 h with DMEM plus fetal bovine serum at 310 K (*VOchrysin free + FBS*). The results are expressed as a percentage of the basal level and represent the mean ± SEM ($n = 9$). All results were significant in comparison with the basal level, $P < 0.01$ (except for 2.5 μM in both cell lines)

A worsening of the deleterious effects of the complex was observed in the MC3T3E1 cells after its replacement by the culture medium supplemented with FBS. That is to say, the cytotoxic effect of the complex persisted after the optimal culture conditions were restored. These conditions are then insufficient to reverse the toxicity triggered by the complex in UMR106 cells and cause a more potent inhibition of the proliferation in the nontransformed osteoblasts. It can also be seen in Fig. 11 that after the removal of the complex, the same inhibitory effect is produced in both cell lines in the additional 24-h culture period under optimal proliferating conditions. Altogether, these results indicate that the inhibition of cell proliferation by the complex is an irreversible phenomenon.

To explain the putative underlying toxicity mechanism, it is worth considering the previously reported results on the selectively generation of free radicals in tumor cells [61]. This may be the reason why there is no difference in the inhibition of cell proliferation under these two conditions in the UMR106 line. In the MC3T3E1 osteoblasts VOchrys also generates a shock, but its effects worsen in the second period of 24-h culture under optimal conditions. In the latter period, the behavior is the same as that observed in the tumor cell line. At a concentration of 100 μM, VOchrys caused 60% inhibition in both cell lines. This shock may be due to the formation of some free radicals, such as superoxide ions which cannot be disproportionated by the complex (see Fig. 8).

Intracellular ROS generation

One of the main mechanisms of cytotoxicity proposed for vanadium and its derivatives is the generation of oxidative stress [62]. In this context, ROS production by VOchrys, chrysin, and VO(IV) was determined in the osteoblast cultures exposed to these substances. ROS generation was estimated by fluorometry using DHR123 as a probe. As mentioned earlier, this probe is a nonfluorescent compound which can detect different ROS, particularly H_2O_2 [63]. In the cells, the DHR123 probe is mainly located in the mitochondria and is oxidized to the fluorescent agent rhodamine 123 in the presence of oxidants. The VOchrys complex depleted ROS levels in the MC3T3E1 cell line at values below the basal level and increased the ROS levels in the tumor cell line at concentrations higher than 75 μM (Fig. 12).

The flavonoid chrysin produced increased quantities of ROS in a dose-dependent manner in both cell lines. On the other hand, VO(IV) exerted an effect similar to that observed for the complex in the tumor cells. In the case of the nontransformed osteoblasts vanadyl(IV) caused a dose-response increase in the ROS level as was previously reported for higher concentrations (1 mM) [64]. Taking into account the VO(IV) effect on MC3T3E1 proliferation (Fig. 10), we can assume that the deleterious effect of this species may be due to the increase of ROS levels in this cell line (Fig. 12). In contrast, in the tumor cell line the proliferation of the cells after the addition of VO(IV) (Fig. 10) was in accordance with the decrease in the ROS levels (Fig. 12). Besides, the increase of oxidative stress induced by chrysin correlates quite well with the inhibition of cell proliferation caused by the ligand in both cell lines. On the other hand, the relationship between these two parameters in the case of VOchrys is very intricate since no evident correlation could be seen. In fact, the complex caused a decrease in the ROS level that can be determined by the DHR123 method in both cell lines (being higher than the basal value only in the UMR106 line at 100 μM) and nevertheless caused inhibition of cell proliferation (Fig. 10). A probable mechanism involved in the deleterious action of the complex may be related to the effect of

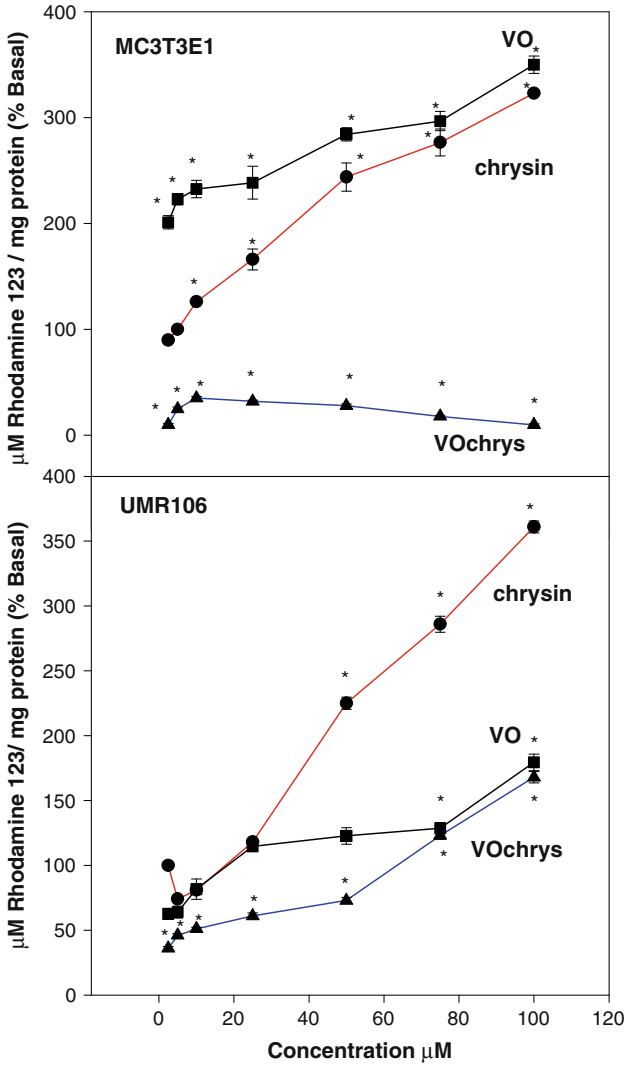

Fig. 12 Effect of VO(IV), chrysin, and VOchrys on dihydrorhodamine 123 (DHR123) oxidation to rhodamine 123. Osteoblast-like cells were incubated at 310 K in the presence of 10 mM DHR123. The values are expressed as a percentage of the basal level for DHR123 oxidation to rhodamine 123 and represent the mean ± SEM ($n = 6$). *Asterisks* significant values in comparison with the basal level ($P < 0.01$)

other free radicals that cannot be detected by the DHR123 probe, such as superoxide radical anion [65–67]. We assume that the complex may induce great levels of this radical in a dose-response manner, which would result in death of both cell lines as was observed in the proliferation assays.

VOchrys induces morphological changes in osteoblasts

The ability of the complex to induce morphological alterations was investigated in both cell lines.

VOchrys-treated cultures displayed changes in their features, as can be seen in Giemsa stained samples, after overnight incubation in a serum-free medium with the addition of different concentrations of VOchrys. Under starved conditions and without the addition of the complex, the control monolayer of MC3T3E1 cells showed the typical fibroblast-like shape (Fig. 13). Nontransformed osteoblasts had well-defined oval and stained nuclei with nucleoli and chromatin granules.

The cytoplasms displayed lamellar expansions that connect each cell with its neighbors. After incubation with 50 μM complex, cells showed a slight cytoplasm condensation and they began to lose the processes between cells. Also, a decrease in the number of cells per field could be observed by light microscopy. Besides, the features of the nuclei were quite well preserved under this experimental condition (Fig. 13). Nevertheless, at 100 μM, a great number of cells died and detached from the culture dishes, so few osteoblasts could be observed. The cytoplasms of the osteoblasts were highly condensed and in many cases their borders were difficult to see. The nuclei maintained their characteristics under this concentration of the complex.

On the other hand, in the tumor cells also some changes in the cell morphology were observed. UMR106 tumoral osteoblasts cultured without addition of the complex (control condition) showed a polygonal morphology with well-stained nuclei which had irregular forms and sizes. The cytoplasms of the cells showed numerous processes that connected each cell with its neighbors (Fig. 13). At 50 μM concentration VOchrys induced an elongation of the osteoblast cytoplasms and the cells became more fusiform in shape. Also a significant decrease in the number of cells per field could be seen (Fig. 13). At 100 μM complex a striking and even more significant diminution in the number of surviving cells was observed.

As a whole, the results of the dose effects of VOchrys on osteoblast morphology parallel the observations in the proliferation studies with the crystal violet bioassay (Fig. 10) for both cell lines.

Conclusions

As part of a project devoted to researching antioxidant flavonoid vanadyl complexes a new complex with chrysin was synthesized and characterized. In ethanolic solution at pH 5 the formation of a 1:2 metal-to-ligand complex was assessed by UV–vis titrations. From EPR studies the presence of a single species (the bis chelate complex) up to a metal-to-ligand ratio of 1:1 could be demonstrated. This species predominates taking into consideration that the chelate effect prevails. It is well known that the stability of a complex containing bis chelating ligands is higher than that of a system containing one chelate and two

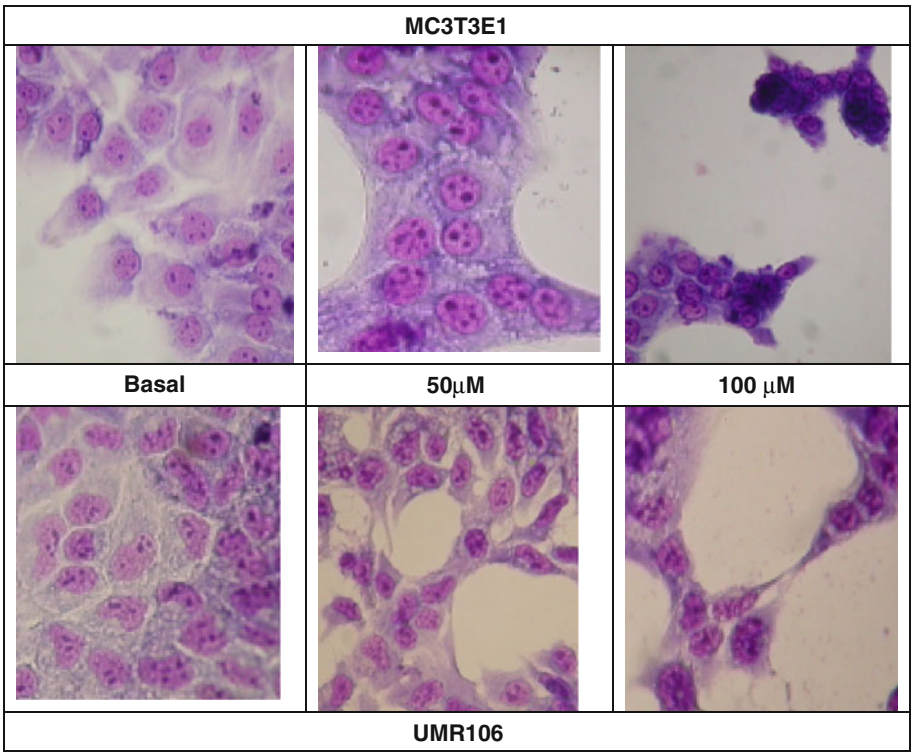

Fig. 13 Effect on cell morphology of the treatment of osteoblatic cell lines with VOchrys. Osteoblasts were incubated for 24 h without drug addition (basal) and with VOchrys (50 and 100 μM). *Top* MC3T3E1 cell line, *bottom* UMR106 cell line (×40)

monodentate ligands. At 1:1 ratio the percentage of the 2:1 ligand-to-metal species is probably higher than that of the 1:1 ligand-to-metal species and uncomplexed vanadium at equilibrium and the inability of EPR spectroscopy to detect the incipient presence of the latter species may be due to the presence of short spin–lattice relaxation times that cause rather large linewidths and consequent low amplitudes for the signal. At lower ligand-to-metal concentrations the concentration of these species is increased and they can be detected by EPR spectroscopy. The antioxidant properties of chrysin are of medium intensity owing to the absence of the 3-hydroxyl group in the skeleton of the compound. The complexation with VO(IV) improved the radical-scavenger activity. The antiproliferative effects both in normal and in tumor cells were determined for the complex and the free ligand, with the effect being more potent in the osteosarcoma-derived cell line. The mechanism of this toxic behavior was explored by means of morphological alterations of the cells and by the generation of ROS. Altogether, the results obtained indicate that the increase in the ROS level detected by the DHR123 probe can explain the deleterious action of chrysin, which is at least partially mediated by OH· and H_2O_2. In the case of VOchrys, with a low level of DHR123-detected ROS, the cytotoxic action may be due to other free radicals such as superoxide anion which was not scavenged by the ligand or by the complex. Since the antiproliferative action of the complex was more pronounced in the osteosarcoma-derived cell line both for the ligand and for the complex, it will be interesting to test these compounds for cancer treatments in further in vivo studies.

Acknowledgments This work was supported by UNLP, CONICET (PIP1125), ANPCyT (PICT 2008-2218) and CICPBA. E.G.F. and S.B.E. are members of the Carrera del Investigador, CONICET. P.A.M.W. is a member of the Carrera del Investigador CICPBA, Argentina. L.N. is a fellowship holder from CONICET.

References

1. Rice-Evans CA, Miller NJ, Paganga G (1996) Free Radic Biol Med 20:933–956
2. Pietta PG (2000) J Nat Prod 63:1035–1042
3. Lu F, Jo YL, Cassady JM (1992) J Nat Prod 55:357–363
4. Habtemariam S (1997) J Nat Prod 60:775–778
5. Sugihara N, Takayuki A, Ohnishi M, Furuno K (1999) Free Radic Biol Med 27:1313–1323
6. Zheng X, Meng WD, Xu Y-Y, Cao JG, Qinga FL (2003) Bioorg Med Chem Lett 13:881–884
7. Koc AN, Silici S, Ayangil D, Ferahbas A, Cankay S (2005) Mycoses 48:205–210
8. Bors W, Heller W, Michel C, Saran M (1990) Methods Enzymol 186:343–355
9. Cárdenas M, Marder M, Blank VC, Roguin LP (2006) Bioorg Med Chem 14:2966–2971
10. Ansari A (2008) Main Group Chem 7:43–56
11. Pusz J, Nitka B, Zielinska A, Wawer I (2000) Microchem J 65:245–253
12. Pusz J, Nitka B (1997) Microchem J 56:373–381
13. Pusz J, Nitka B, Kopacz S, Korenman YI (2003) Russ J Gen Chem 73:634–637

14. Onishi M (1988) Photometric determination of traces of metals, part II, 4th edn. Wiley, New York
15. Yamaguchi T, Takamura H, Matoba TC, Terao J (1998) Biosci Biotechnol Biochem 62:1201–1204
16. Pellegrini RN, Proteggente A, Pannala A, Yang M, Rice-Evans C (1999) Free Radic Biol Med 26:1231–1237
17. Gorinstein S, Moncheva S, Katrich E, Toledo F, Arancibia P, Goshev I, Trakhtenberg S (2003) Mar Pollut Bull 46:1317–1325
18. Kuo CC, Shih M, Kuo Y, Chiang W (2001) J Agric Food Chem 49:1564–1570
19. Halliwell B, Gutteridge JMC, Aruoma OI (1987) Anal Biochem 165:215–219
20. Zhong Z, Ji X, Xing R, Liu S, Guo Z, Chen X, Li P (2007) Bioorg Med Chem 15:3775–3782
21. Cortizo AM, Etcheverry SB (1995) Mol Cell Biochem 145:97–102
22. Krejsa CM, Nadler SG, Esselstyn JM, Kavanagh TJ, Ledbetter JA, Schieven GL (1997) J Biol Chem 272:11541–11549
23. Bradford M (1976) Anal Biochem 72:248–254
24. Sálice VC, Cortizo AM, Gómez Dumm CL, Etcheverry SB (1999) Mol Cell Biochem 198:119–128
25. Engelmann MD, Hutcheson R, Cheng IF (2005) J Agric Food Chem 53:2953–2960
26. Castro GT, Ferretti FH, Blanco SE (2005) Spectrochim Acta A 62:657–665
27. Chasteen ND (1981) Vanadyl (IV) spin probes, inorganic and biochemical aspects. In: Berliner LJ, Reuben J (eds) Biological magnetic resonance, vol 3. Plenum, New York
28. Chruscinska E, Garribba E, Micera G, Panzanelli A (1999) J Inorg Biochem 75:225–232
29. Buglyó P, Kiss E, Fábián I, Kiss T, Sanna D, Garribba E, Micera G (2000) Inorg Chim Acta 306:174–183
30. Hanson GR, Sun Y, Orvig C (1996) Inorg Chem 35:6507–6512
31. Amin SS, Cryer K, Zhang B, Dutta SK, Eaton SS, Anderson OP, Miller SM, Reul BA, Brichard SM, Crans DC (2000) Inorg Chem 39:406–416
32. Stewart CP, Porte AL (1972) J Chem Soc Dalton Trans 1661–1666
33. Caravan P, Gelmini L, Glover N, Geoffrey Herring F, Li H, McNeill JH, Rettig SJ, Setyawati IA, Shuter E, Sun Y, Tracey AS, Yuen VG, Orvig C (1995) J Am Chem Soc 117:12759–12770
34. Kiss T, Jakush T, Kilyén M, Kiss E, Lakatos A (2000) Polyhedron 19:2389–2401
35. Delgado TC, Tomaz AI, Correia I, Costa Pessoa J, Jones JG, Geraldes CFGC, Margarida M, Castro CA (2005) J Inorg Biochem 99:2328–2339
36. McPhail DB, Goodman BA (1987) J Chem Soc Faraday Trans 83:3627–3633
37. Costa Pessoa J, Cavaco I, Correia I, Tomaz I, Duarte T, Matias PM (2000) J Inorg Biochem 80:35–39
38. Cornman CR, Zovinka EP, Boyajian YD, Geiser-Bush KM, Boyle PD, Sing P (1995) Inorg Chem 34:4213–4219
39. Dörnyei A, Marcão S, Costa Pessoa J, Jakusch T, Kiss T (2006) Eur J Inorg Chem 18:3614–3621
40. Lin-Vien D, Colthup NB, Fateley WG, Grasselli JC (1991) The handbook of infrared and Raman characteristic frequencies of organic molecules. Academic Press, Boston
41. Nyquist RA (ed) (2001) Interpreting infrared, Raman, and nuclear magnetic resonance spectra, chap 7. Elsevier, Amsterdam
42. Corredor C, Teslova T, Vega Cañamares M, Chen Z, Zhang J, Lombardi JR, Leona M (2009) Vibr Spectrosc 49:190–195
43. Ferrer EG, Salinas MV, Correa MJ, Naso L, Barrio DA, Etcheverry SB, Lezama L, Rojo T, Williams PAM (2006) J Biol Inorg Chem 11:791–801
44. Etcheverry SB, Ferrer EG, Naso L, Rivadeneira J, Salinas V, Williams PAM (2008) J Biol Inorg Chem 13:435–447
45. Nuopponena M, Willför S, Jääskeläinen AS, Vuorinen T (2004) Spectrochim Acta A 60:2963–2968
46. Bencini A, Gatteschi D (1990) EPR of exchange coupled systems. Springer, Berlin
47. Unamuno I, Gutiérrez-Zorrilla JM, Luque A, Román P, Lezama L, Calvo R, Rojo T (1998) Inorg Chem 37:6452–6460
48. Harris GK, Willcox JK, Catignani GL (2004) J Food Biochem 28:337–349
49. Burda S, Oleszek W (2001) J Agric Food Chem 49:2774–2779
50. Harman DJ (1956) Gerontology 11:289–300
51. Warma SD, Devamanoharan PS, Morris SM (1995) Crit Rev Food Sci Nutr 35:111–129
52. Cos P, Ying L, Calomme M, Hu JP, Cimanga K, Van Poel B, Pieters L, Vlietinck AJ, Vanden Berghe D (1998) J Nat Prod 61:71–76
53. Yu BP (1994) Physiol Rev 74:139–162
54. Adams JD, Odunze IN (1991) Free Radic Biol Med 10:161–169
55. Hall ED (1994) Free radicals in central nervous system injury. In: Rice-Evans C, Burdon RH (eds) Free radical damage and its control. Elsevier, Amsterdam, pp 113–130
56. Edgington DE (1994) Biotechnology 12:37–39
57. Ames BN, Shigenaga MK, Hagen TM (1993) Proc Natl Acad Sci USA 90:7915–7922
58. Halliwell B, Gutteridge JMC (1986) Arch Biochem Biophys 246:501–514
59. Ko FN, Cheng ZJ, Lin CN, Teng CM (1998) Free Radic Biol Med 25:160–168
60. Cheng Z, Ren J, Li Y, Chang W, Chen Z (2002) Bioorg Med Chem 10:4067–4073
61. Das UN, Huang YS, Bēgin ME, Ells G, Horrobin DF (1987) Free Radic Biol Med 3:9–14
62. Evangelou AM (2002) Crit Rev Oncol Hematol 42:249–265
63. Capella MAM, Capella LS, Valente RC, Gefé M, Lopes AG (2007) Cell Biol Toxicol 23:413–420
64. Cortizo AM, Bruzzone L, Molinuevo S, Etcheverry S (2000) Toxicology 147:89–99
65. Schuessel K, Frey C, Jourdan C, Keil U, Weber CC, Müller-Spahn F, Müller WE, Eckert A (2006) Free Radic Biol Med 40:850–862
66. Masaki H, Sakurai H (1995) Photomed Photobiol 17:121–124
67. Qin Y, Lu M, Gong X (2008) Cell Biol Int 32:224–228